2D Layered metal–organic frameworks built using a hexanuclear metallamacrocycle and an octanuclear metallamacrocycle as supramolecular building blocks†

Dohyun Moon, Jiheh Song and Myoung Soo Lah*

Received 5th August 2008, Accepted 14th November 2008
First published as an Advance Article on the web 19th January 2009
DOI: 10.1039/b813603c

Two different 2D layered metal–organic frameworks (MOFs) have been prepared using a hexanuclear manganese metallamacrocycle and an octanuclear manganese metallamacrocycle as supramolecular building blocks *via* a simple change of the solvent used and/or addition of a templating agent. While the sheets in the 2D MOF $[Mn_6(pshz)_6(bpea)_2(dma)_2]_n$, **2** (where, $pshz^{3-}$ is *N*-propionylsalicylhydrazidate, bpea is 1,2-bis(pyridyl)ethane, and dma is *N,N*-dimethylacetamide), built based on a hexanuclear metalladiazamacrocycle are in a staggered orientation, the sheets in the 2D MOF $[Mn_8(pshz)_8(bpea)_2(dma)_4]_n$, **3**, built based on an octanuclear metalladiazamacrocycle are in an eclipsed orientation. However, both MOFs have the same 3-connected 4.8^2 network topology.

Introduction

A node-and-linker approach, where a metal ion is usually used as a node and an organic ligand as a linker, is one of the most efficient and promising strategies for the construction of diverse metal–organic frameworks (MOFs).[1] Although the nodality and geometry of a metal center can be controlled based on the coordination preference of the metal ion and/or the stability of the ligands coordinated to the metal ion, the diversity of nodes is still limited because of the inherent limitation of possible geometries in a simple metal center when the metal ion is used as a node in the formation of MOFs. Metal–organic clusters as secondary building units (SBUs) can extend their utility in the node-and-linker approach because the clusters can also serve as a node of high rigidity with various connectivities and geometries for network constructions.[2]

Supramolecular building blocks (SBBs), which are the structural entities that can exist as distinctive molecular entities in solution, could be employed as alternative nodes with various connectivities and unusual geometries.[3] In addition, the SBB approach provides an additional advantage for the construction of MOFs over the conventional approach because the properties of the resulting MOFs can be controlled at the more predictable supramolecular level than at the less predictable molecular level.[4,5] Diaza-bridged hexanuclear manganese metallamacrocycles, which have a replaceable solvent site at every metal center in the macrocyclic ring, have been used as a supramolecular node for the construction of various MOFs.[5–7] Depending on the conditions, a hexanuclear manganese metallamacrocycle has been used as either a rectangular tetratopic node, which leads to helical coordination nets of the SBBs,[5–7] or an octahedral hexatopic node, which leads to a simple cubic net.[7] Even though several diaza-bridged metallamacrocycles of higher nuclearities have already been reported, none of them were used as an SBB in the construction of MOFs.[7,8]

In this study, we have synthesized two new 2D layered MOFs using either a hexanuclear metalladiazamacrocycle or an octanuclear metalladiazamacrocycle as an SBB depending on the reaction conditions (Scheme 1). The nuclearity of the SBBs and/or their connectivity in the resulting MOFs can be modulated based on the solvents used and the template molecule present.

Results and discussion

Slow diffusion of manganese(II) acetate into a dma solution of H_3pshz and bpea led to the simultaneous formation of two different shapes of dark brown crystals, a needle-shaped crystal, **2**, as a minor form and a block-shaped crystal, **3**, as the major form. Structural analysis of a dark brown needle-shaped crystal showed that **2** is a 2D layered MOF, $[Mn_6(pshz)_6(bpea)_2(dma)_2]_n$, (where, $pshz^{3-}$ is *N*-propionylsalicylhydrazidate, bpea is 1,2-bis(pyridyl)ethane, and dma is *N,N*-dimethylacetamide) built based on the 18-membered hexanuclear manganese metallamacrocycle, $[Mn_6(pshz)_6]$, as a tetratopic SBB linked by an exo-bidentate bridging ligand, bpea (Fig. 1 and S1†). The hexanuclear manganese metallamacrocyclic unit in **2** is very similar to the reported manganese metallamacrocycle, $[Mn_6(pshz)_6(dmf)_6]$ (where dmf is *N,N*-dimethylformamide).[8b] Only four of the six exchangeable solvent sites on the hexanuclear SBB (*h*SBB) were replaced by the ditopic linker ligand, bpea (Fig. 1a). This kind of tetratopic nodality is similar to that observed in the reported 3D MOF, $[Mn_6(pshz)_6(bpea)_2(dmf)_2]_n$, **1**, constructed using the same *N*-propionylsalicylhydrazidate-based *h*SBB in dmf solvent (Scheme 1).[5,7] Although the same *h*SBB has been used and the same nodality was employed, a simple solvent change from dmf to dma led to a MOF of

---

Department of Chemistry and Applied Chemistry, College of Science and Technology, Hanyang University, Ansan, Kyunggi-do, 426-791, Korea. E-mail: mslah@hanyang.ac.kr; Fax: +82-31-436-8100; Tel: +82-31-400-5496

† Electronic supplementary information (ESI) available: Crystallographic data in CIF, ORTEP drawings, crystallographic analysis tables, and TGA data for **2** and **3**. CCDC reference numbers 697383 and 697384. For ESI and crystallographic data in CIF or other electronic format see DOI: 10.1039/b813603c

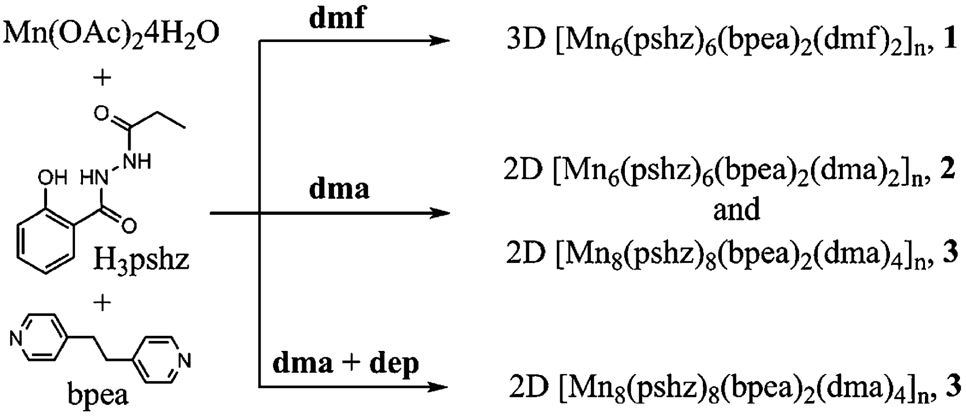

Scheme 1 Schematic diagram showing solvent and guest dependence on the preparation of MOFs.

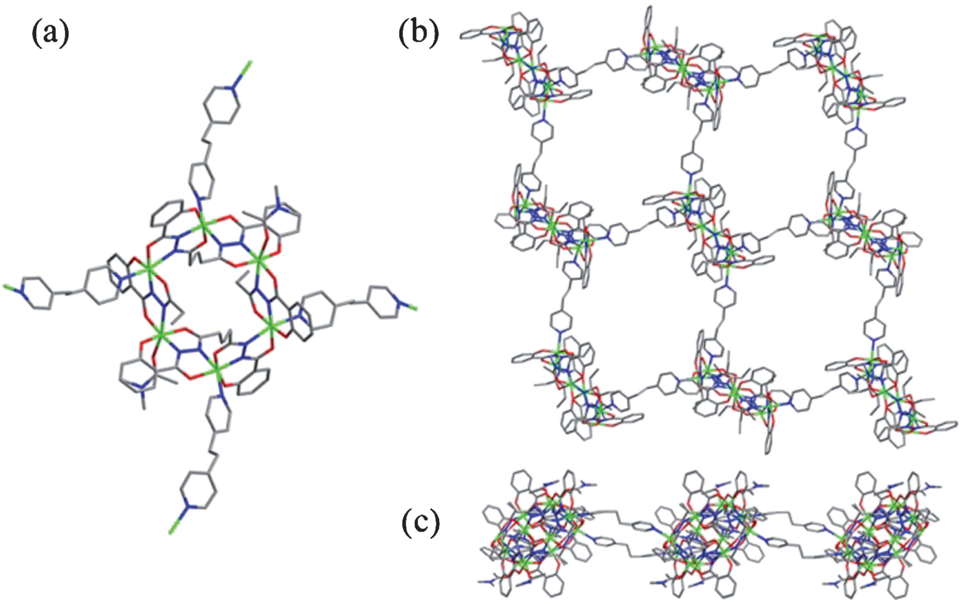

Fig. 1 Stick diagrams of the 2D layered MOF, $[Mn_6(pshz)_6(bpea)_2(dma)_2]_n$, **2**. Key: Mn (green), N (blue), O (red), C (gray). (a) A stick diagram of an *h*SBB with four solvent molecules substituted with bpea linkers. (b) A top view of a 2D layer showing *h*SBBs interlinked *via* bpea linkers. (c) A side view of the 2D layered structure.

different network topology, the 2D layered network, $[Mn_6(pshz)_6(bpea)_2(dma)_2]_n$, **2** (Fig. 1 and 2). The difference was reflected in the orientation of the bridging ligand, bpea, relative to that of the *h*SBB in the 2D layered network, **2**. The bridging ligand in the 2D network, **2**, (Fig. 3a) is in a less puckered orientation compared with that of the ligand in the 3D network, **1** (Fig. 3b). The *h*SBB in the 2D layered structure has acted as a rectangular tetratopic node. Network **2** is a 2D MOF with a 3-connected 4.8^2 network topology (Fig. 2c).[9] When the hexanuclear macrocyclic unit was reduced to a planar rectangular 4-connected vertex, the net could be further simplified to a 4-connected 4^4 net (Fig. 2d). Extensive inter-sheet interactions were observed in the network, **2** (Table S3†). Weak CH···O hydrogen-bonding interactions were observed between a pyridyl hydrogen atom of the bpea linker and a phenolate oxygen atom of a pshz ligand, and between a hydrogen atom of the phenolate group and a symmetry-related phenolate oxygen atom. The *N*-methyl group of a ligated dma molecule participates in a weak CH···π interaction with the phenolate part of the ligand in the adjacent layer. These weak interactions contribute to the stacking of the 2D sheets in a staggered orientation (Fig. 2). Even though the 2D sheets were staggered, there still remains some solvent-accessible space because of the corrugated nature of the 2D sheet in network **2**. The solvent-accessible volume of network **2** was estimated by the PLATON program[10] to be 23.5% (2619 Å^3) of the total crystal volume.

Dark brown block-shaped single crystals, **3**, were obtained as the major product but always with some network **2** crystals when a manganese(II) acetate was slowly diffused into a dma solution of H_3pshz and bpea. However, reaction under identical conditions but with diethyl phthalate (dep) as a templating or potential guest molecule led to **3** as the sole product (Scheme 1). The crystal structure analysis of **3** (Fig. S2†) showed that the network is again a 2D layered MOF, $[Mn_8(pshz)_8(bpea)_2(dma)_4]_n$, but the

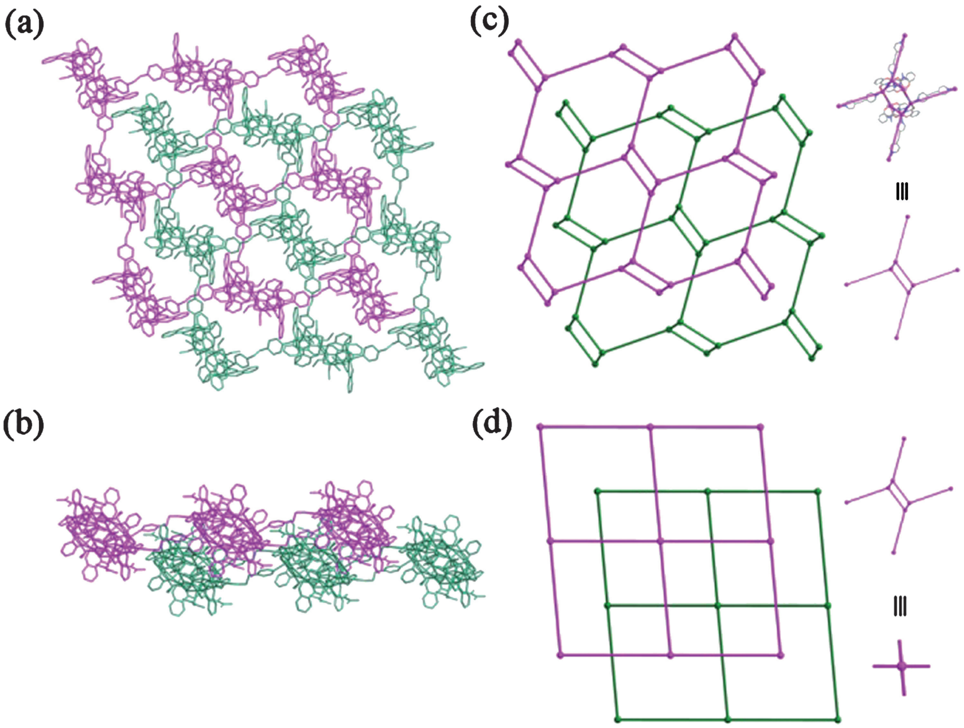

Fig. 2 A packing diagram of **2**, and its schematic diagrams and their network topologies. (a) A packing diagram of network **2** shows two stacked 2D layers in a staggered orientation, where the two layers are differentiated *via* different colors, pink and green. (b) A side view of the packing diagram of **2**. (c) A schematic diagram representing the connectivity of the metal centers. When the metal center linked is considered as a trinode, the net could be described as a 3-connected 4.8^2 net. (d) When the metallamacrocycle, presented as a rectangular shape, is further reduced to a rectangular node, the net can be described as a staggered 4-connected 4^4 net.

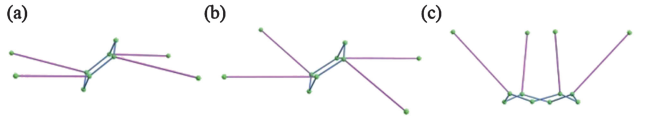

Fig. 3 The orientations of the bridging bpea ligands relative to the metallamacrocycles, SBBs, in the MOFs. The green ball and blue stick represent the manganese ion and pshz ligand in the metallamacrocycles, respectively, and the pink stick represents a linker ligand, bpea. (a) Four bpea linkers are in a less puckered orientation relative to *h*SBB in the 3D network, **1**. (b) Four bpea linkers are in a more puckered orientation relative to *h*SBB in the 2D network, **2**. (c) All four bpea linkers of the *o*SBB in the 2D network **3** are oriented towards the same facial direction.

SBB employed is an octanuclear metallamacrocycle, which is observed for the first time as an SBB in MOFs. The octanuclear manganese metallamacrocyclic unit in **3** is similar to the reported manganese metallamacrocycle, $[Mn_8(2\text{-mshz})_8(dmso)_8]$ (where, 2-mshz^{3-} is *N*-(2,2-dimethylpropanoyl)salicylhydrazidate and dmso is dimethylsulfoxide).[8c] The alternating four replaceable solvent sites out of eight in the octanuclear SBB (*o*SBB) were substituted by the exo-bidentate ligand, bpea, in the network. This kind of alternating substitution of the solvent molecules orients all bpea linkers on the same facial side of the metallamacrocycle (Fig. 3c and 4a), which leads to a corrugated 2D layered structure based on the 24-membered octanuclear manganese metallamacrocycle, $[Mn_8(pshz)_8]$, as an *o*SBB (Fig. 4b and 4c). When the metal center linked in network **3** is considered as a trinode (Fig. 5c), the net topology of **3** is a 3-connected 4.8^2 net, as in network **2**. The *o*SBB in network **3** has acted as a square tetratopic node. When the octanuclear macrocyclic unit was reduced to a square planar 4-connected vertex, the net could be further simplified to a 4-connected 4^4 net (Fig. 5d). In network **3**, the corrugated 2D sheets are stacked in an eclipsed orientation, which generates 3D solvent channels (Fig. 5a and b).

The ligated dma molecules in network **3** are involved in inter-sheet interactions *via* two-way $\pi\cdots\pi$ stacking interactions (~3.66 Å average displacement) with phenolic benzene groups of the ligand (Fig. 6 and Table S4†). A total of eight $\pi\cdots\pi$ stacking interactions per *o*SBB leads to the corrugated 2D sheets in an eclipsed orientation. One thing to mention is that an octanuclear metallamacrocyclic unit having a flexible linear *N*-acyl salicylhydrazide was only obtained when dma was used as the solvent. This suggests that the dma involved in the $\pi\cdots\pi$ stacking interaction plays an important role in the formation of the *o*SBB. The fact that network **3** is only obtained as the sole product in the presence of dep as a templating agent suggests that dep also plays some role in the formation of network **3**. However, it is still difficult to elucidate its exact role in the network formation because of the absence of structural information regarding dep. The dep molecules are neither incorporated as a framework component, nor ordered in the solvent channel.

To assess the thermal stability of the networks, thermogravimetric analyses were carried out using a heating rate of 10 °C min^{-1} in air. As shown in Fig. S3,† the TGA curve of network **2**

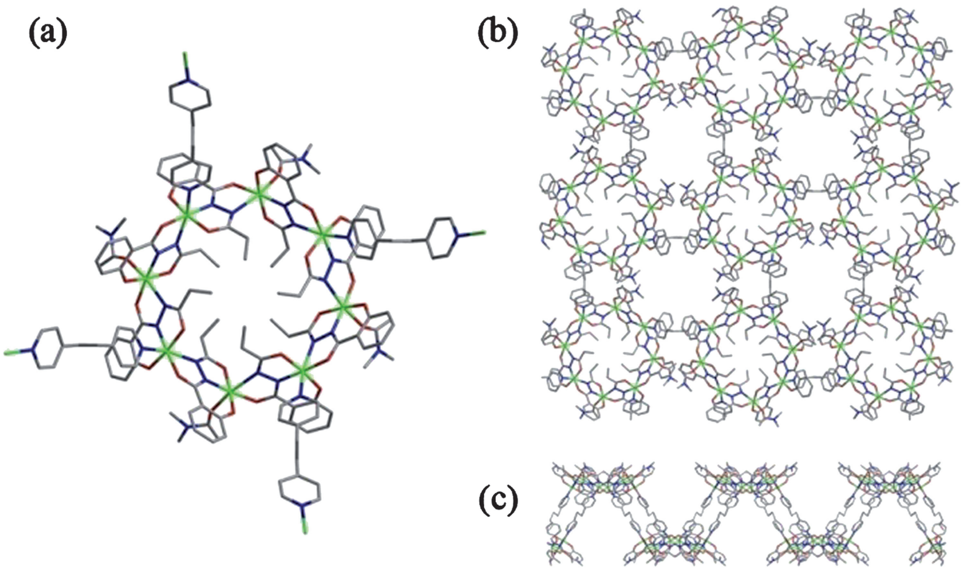

Fig. 4 Stick diagrams of the 2-D layered MOF, $[Mn_8(pshz)_8(bpea)_2(dma)_4]_n$, **3**. Key: Mn (green), N (blue), O (red), C (gray). (a) A stick diagram of an *o*SBB with four solvent molecules substituted with bpea linkers. (b) A top view of a 2D layer showing *o*SBBs interlinked *via* bpea linkers. (c) A side view of the 2D layered structure.

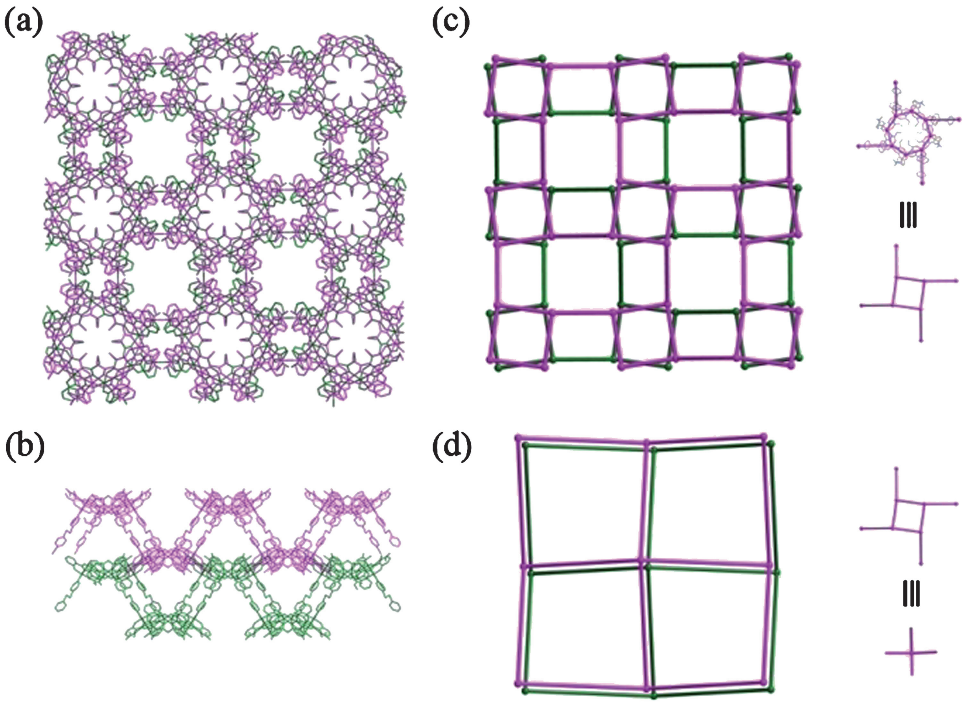

Fig. 5 A packing diagram of **3**, and its schematic diagrams and their network topologies. (a) A packing diagram of network **3** shows two stacked 2D layers in an eclipsed orientation, where the two layers are differentiated *via* different colors, pink and green. (b) A side view of the packing diagram of **2** showing the corrugated nature of its 2D layered structure. (c) A schematic diagram representing the connectivity of the metal centers. When the metal center linked is considered as a trinode, the net could be described as a 3-connected 4.8^2 net. (d) When the metallamacrocycle, presented as a square shape, is further reduced to a square node, the net can be described as an eclipsed 4-connected 4^4 net.

exhibited two significant weight losses. The first weight loss occurred between 50 and 250 °C, which was attributed to the loss of solvent molecules. The decomposition of network **2** occurs in the temperature range 340–450 °C. Network **3** exhibited a similar TGA characteristic, two-step weight loss (Fig. S4†). The decomposition of network **3** occurs in the temperature range 255–450 °C. However, both MOFs are unstable when the solvent in the channel is removed. The amorphous powder X-ray

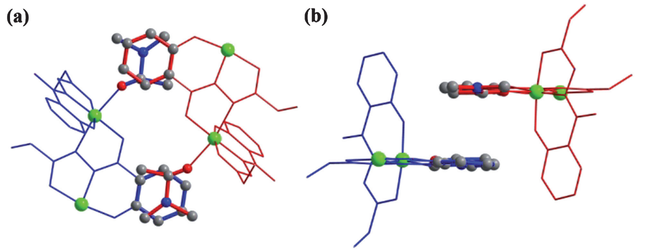

Fig. 6 A ball-and-stick diagram showing a pair of two-way inter-sheet $\pi\cdots\pi$ stacking interactions observed between phenolic benzene groups of the ligands and dma molecules ligated in the ring metal centers of the *o*SBB, where the π electrons of the amide residue of the dma are responsible for the $\pi\cdots\pi$ interaction. The two sheets are differentiated using blue and red lines, respectively, and the residues involved in the $\pi\cdots\pi$ stacking interactions are presented in a ball-and-stick drawing. (a) A top view. (b) A side view. Key: Mn (green ball), N (blue ball), O (red ball), C (dark gray ball).

diffraction patterns of the samples with the solvent removed suggest the collapse of the networks in the absence of the solvents.

Experimental

Materials and general methods

The following were used as received with no further purification: manganese(II) acetate tetrahydrate, bpea, dep from Aldrich, Inc.; dma from Junsei. *N*-propionylsalicylhydrazide (H_3pshz) was synthesized as described previously.[8b] Elemental analysis was performed at the Organic Chemistry Research Center in Sogang University (Korea) using a TE Flash EA 1112 series elemental analyzer. Infrared spectra were recorded using KBr pellets in the range 4000–400 cm^{-1} using a Varian FTS 1000 FT-IR spectrometer. Thermogravimetric analysis was performed on a Scinco Simultaneous Thermal Analyzer (STA) S-1000 with a heating rate of 10 °C min^{-1} between ambient temperature and 550 °C.

Preparation of complexes

[Mn_6(pshz)$_6$(bpea)$_2$(dmf)$_2$] (1). 1 was synthesized as described previously.[5]

[Mn_6(pshz)$_6$(bpea)$_2$(dma)$_2$] (2) and [Mn_8(pshz)$_8$(bpea)$_2$(dma)$_4$] (3). A 0.104 g (0.499 mmol) sample of H_3pshz was dissolved in 15 mL of dma solution. Then, 0.092 g (0.499 mmol) of bpea was added to the solution and stirred for 5 min. When all ligands were dissolved completely, 0.123 g (0.502 mmol) of manganese(II) acetate tetrahydrate was added to the solution without stirring. The solution was allowed to stand for 20 d, whereupon dark brown needle-shaped crystals as a minor form, **2**, and dark brown rectangular-shaped crystals, **3**, as a major form were simultaneously obtained in the same batch. The mixed crystals were vacuum dried (0.143 g, 81.7% yield based on metal ion used). Elemental analysis results for mixed products are as follows. Found: C, 52.51; H, 4.77; N, 12.06%. IR (cm^{-1}, KBr pellet): 3456, 3062, 2972, 2936, 2877, 1601, 1567, 1504, 1442, 1406, 1356, 1323, 1246, 1109, 1014, 899, 857, 815, 758, 686, 593, 544, and 422.

[Mn_8(pshz)$_8$(bpea)$_2$(dma)$_4$] (3). 7.0 mL of dep was added to 10 mL of dma. A 0.104 g (0.499 mmol) sample of H_3pshz was dissolved in the solution. Then, 0.092 g (0.499 mmol) of bpea was added to the solution and stirred for 5 min. When all ligands were dissolved completely, 0.123 g (0.502 mmol) of manganese(II) acetate tetrahydrate was added to the solution without stirring. The solution was allowed to stand for 5 d, whereupon dark brown rectangular-shaped crystals, **3**, were obtained as the sole product. The crystals were soaked in fresh dma for several hours, filtered, and vacuum dried (0.182 g, 74.6% yield). Elemental analysis calcd for [Mn_8(pshz)$_8$(bpea)$_2$(dma)$_4$] ($Mn_8C_{120}H_{132}N_{24}O_{28}$) (fw = 2796.47): C, 51.49; H, 4.76; N, 12.02%. Found: C, 51.50; H, 4.82; N, 12.04%. IR (cm^{-1}, KBr pellet) for the crystals vacuum dried without pre-soaking in fresh dma: 3434, 3062, 2974, 2937, 2877, 1721, 1602, 1569, 1504, 1442, 1406, 1356, 1324, 1246, 1109, 1015, 899, 857, 814, 757, 687, 593, 544, and 421. The IR spectrum of **3** looks the same as that of a mixture of **2** and **3** crystals except for an additional peak at 1721 cm^{-1} for the carbonyl group of diethyl phthalate.

Crystallographic details

[Mn_6(pshz)$_6$(bpea)$_2$(dma)$_2$], 2. The crystal was coated with paratone oil because the crystal loses its crystallinity on exposure to air. The diffraction data were measured with synchrotron radiation on a 4AMXW ADSC Quantum-210 detector with a silicon double-crystal monochromator at the Pohang Accelerator Laboratory, Korea. The ADSC Quantum-210 ADX program[11] was used for data collection, and HKL2000 (Ver. 0.98.698a)[12] was used for cell refinement, reduction, and absorption correction. The structures were solved by direct methods and refined by full-matrix least-squares calculations

Table 1 Crystallographic data and structure refinement summary

	2	3
Chemical formula	$Mn_6C_{104}H_{120}N_{21}O_{24}$	$Mn_8C_{165}H_{233.25}N_{35.25}O_{39.25}$
Formula weight	2377.85	3778.14
Crystal system	Monoclinic	Tetragonal
Space group	*C*2/*c*	*P*4/*ncc*
T/K	100(2)	173(2)
Wavelength, λ/Å	0.80000	0.71073
a/Å	16.675(3)	26.988(3)
b/Å	28.710(6)	26.988(3)
c/Å	23.663(5)	29.158(5)
α/°	90.00	90.00
β/°	100.23(3)	90.00
γ/°	90.00	90.00
V/Å^3	11148(4)	21238(5)
Z	4	4
D/g cm^{-3}	1.417	1.182
μ/mm^{-1}	0.726	0.531
$2\theta_{max}$/°	60.8	44
F(000)	4932	7936
Reflns measured	39781	42577
Obsd reflns	11692	6531
R_{int}	0.0598	0.0990
$R1^a/wR2^b$ $(I > 2\sigma(I))$	0.0646/0.1823	0.0837/0.2243

[a] $R1 = \sum(|F_0| - |F_0|)/\sum|F_0|$. [b] $wR2 = [\sum[w(F_0^2 - F_0^2)^2]/\sum w(F_0^2)^2]^{2/2}$.

with the SHELXTL-PLUS (Ver. 5.1) software package.[13] Two unligated dma molecules and a water molecule were found in the difference Fourier map and included in the subsequent least-squares refinement, where a dma molecule and the water molecule are statically disordered around a crystallographic two-fold axis. All non-hydrogen atoms were refined anisotropically; hydrogen atoms, excluding the hydrogen atoms attached to the disordered dma molecule and the water molecule, were assigned isotropic displacement coefficients $U(\mathrm{H}) = 1.2U$ (C) or $1.5U(\mathrm{C_{methyl}})$, and their coordinates were allowed to ride on their respective atoms. Refinement of the structure converged at a final $R1 = 0.0646$, and $wR2 = 0.1823$ for 10 901 reflections with $I > 2\sigma(I)$, $R1 = 0.0675$, $wR2 = 0.1849$ for all reflections. The largest difference peak and hole were 1.381 and -0.840 e Å^{-3}, respectively. Crystal and intensity data are given in Table 1.

[$\mathbf{Mn_8(pshz)_8(bpea)_2(dma)_4}$], 3. The crystal was coated with paratone oil because the crystal loses its crystallinity on exposure to air. The diffraction data were measured with Mo Kα radiation on a Brukers SMART CCD equipped with a graphite-crystal, incident-beam monochromator. The SMART and SAINT software packages[14] were used for data collection and integration, respectively. The collected data were corrected for absorbance using SADABS[15] based upon Laue symmetry using equivalent reflections. Structures were solved by direct methods and refined by full-matrix least-squares calculations with the SHELXTL-PLUS (ver. 5.1) software package.[13] All non-hydrogen atoms were refined anisotropically; hydrogen atoms were assigned isotropic displacement coefficients $U(\mathrm{H}) = 1.2U$ (C) or $1.5U$ ($\mathrm{C_{methyl}}$), and their coordinates were allowed to ride on their respective atoms. All propionyl side chains of the ligands were statically disordered. The refinement converged to $R1 = 0.1722$, and $wR2 = 0.4286$ for 42 577 reflections of $I > 2\sigma(I)$. Structure refinement after modification of the data for the non-coordinate lattice solvent molecules with the SQUEEZE routine of PLATON (9858 Å^3, 46.4% of the crystal volume, 2167 solvent electrons ($\sim$45 dma molecules) per unit cell)[10] led to better refinement and data convergence. Refinement of the structure converged at a final $R1 = 0.0837$, and $wR2 = 0.2243$ for 2882 reflections with $I > 2\sigma(I)$; $R1 = 0.1522$, and $wR2 = 0.2523$ for all reflections. The largest difference peak and hole were 0.616 and -0.261 e Å^{-3}, respectively. Crystal and intensity data are given in Table 1.

Conclusions

We have synthesized two 2D layered MOFs using manganese(II) acetate, a pentadentate bridging ligand, $\mathrm{H_3pshz}$, and an exobidentate ligand, bpea, where either a hexanuclear manganese metallamacrocycle or an octanuclear manganese metallamacrocycle has been used as an SBB. In contrast to the self-assembly of the 3D MOF, **1**,[5] under the same reaction conditions but with dmf as the solvent, a simple change of the solvent dmf to dma led to a 2D layered MOF, **2**. This is built based on a hexanuclear manganese metallamacrocycle as a rectangular tetratotic SBB as a minor product along with another 2D layered MOF, **3**, based on an octanuclear manganese metallamacrocycle as a square-planar tetratotic SBB as the major product. Addition of dep to the reaction solution as a templating agent resulted in network **3** as the sole product. Although the topology of both 2D networks **2** and **3**, a 3-connected 4.8^2 net, is the same, the 2D sheets in **2** are in a staggered orientation, and the 2D sheets in **3** are in an eclipsed orientation. The solvent dma, ligated in the metallamacrocyclic building block, seems to play a key role determining the final network structure *via* participation in the inter-sheet interaction in both networks **2** and **3**.

In this study, we have demonstrated the preparation of two different 2D MOFs based on an SBB approach. In this approach, an MOF containing an octanuclear metallamacrocycle as a new SBB has been obtained unexpectedly for the first time *via* small changes in the reaction conditions. This work shows that we still have a long way to go before we predict the final MOF from the building components or reaction conditions.

Acknowledgements

This work was supported by KRF (KRF-2005-070-C00068), KOSEF (R01-2007-000-10167-0), and CBMH. The authors also acknowledge PAL for beam line use (2008-2041-03).

References

1 (*a*) M. O'Keeffe, M. Eddaoudi, H. Li, T. Reineke and O. M. Yaghi, *J. Solid State Chem.*, 2000, **152**, 3; (*b*) S. R. Batten and R. Robson, *Angew. Chem., Int. Ed.*, 1998, **37**, 1460; (*c*) S. Kitagawa, R. Kitaura and S.-i. Noro, *Angew. Chem., Int. Ed.*, 2004, **43**, 2334; (*d*) C. A. Williams, A. J. Blake, P. Hubberstey and M. Schröder, *Chem. Commun.*, 2005, 5435; (*e*) K. Biradha, M. Sarkar and L. Rajput, *Chem. Commun.*, 2006, 4169; (*f*) M. J. Zaworotko, *Cryst. Growth Des.*, 2007, **7**, 4.

2 (*a*) M. Eddaoudi, D. B. Moler, H. Li, B. Chen, T. M. Reineke, M. O'Keeffe and O. M. Yaghi, *Acc. Chem. Res.*, 2001, **34**, 319; (*b*) F. A. Cotton, C. Lin and C. A. Murillo, *Acc. Chem. Res.*, 2001, **34**, 759; (*c*) S. S.-Y. Chui, S. M.-F. Lo, J. P. H. Charmant, A. G. Orpen and I. D. Williams, *Science*, 1999, **283**, 1148; (*d*) J. Kim, B. Chen, T. M. Reineke, H. Li, M. Eddaoudi, D. B. Moler, M. O'Keeffe and O. M. Yaghi, *J. Am. Chem. Soc.*, 2001, **123**, 8239; (*e*) S. A. Bourne, J. Lu, A. Mondal, B. Moulton and M. J. Zaworotko, *Angew. Chem., Int. Ed.*, 2001, **40**, 2111; (*f*) C. Serre, F. Millange, S. Surblé and G. Férey, *Angew. Chem., Int. Ed.*, 2004, **43**, 6286; (*g*) S. Surblé, F. Millange, C. Serre, G. Férey and R. I. Walton, *Chem. Commun.*, 2006, 1518; (*h*) O. M. Yaghi, M. O'Keeffe, N. W. Ockwig, H. K. Chae, M. Eddaoudi and J. Kim, *Nature*, 2003, **423**, 705; (*i*) M. Casarin, C. Corvaja, C. D. Nicola, D. Falcomer, L. Franco, M. Monari, L. Pandolfo, C. Pettinari and F. Piccinelli, *Inorg. Chem.*, 2005, **44**, 6265; (*j*) E.-C. Yang, J. Li, B. Ding, Q.-Q. Liang, X.-G. Wang and X.-J. Zhao, *CrystEngComm*, 2008, **10**, 158; (*k*) S. Ma, X.-S. Wang, E. S. Manis, C. D. Collier and H.-C. Zhou, *Inorg. Chem.*, 2007, **46**, 3432; (*l*) H. Chun, H. Jung, G. Koo, H. Jeong and D.-K. Kim, *Inorg. Chem.*, 2008, **47**, 5355; (*m*) A. Thirumurugan and S. Natarajan, *Cryst. Growth Des.*, 2006, **6**, 983; (*n*) H. K. Chae, D. Y. Siberio-Pérez, J. Kim, Y. Go, M. Eddaoudi, A. J. Matzger, M. O'Keeffe and O. M. Yaghi, *Nature*, 2004, **427**, 523; (*o*) B. Chen, M. Eddaoudi, S. T. Hyde, M. O'Keeffe and O. M. Yaghi, *Science*, 2001, **291**, 1021; (*p*) H. Li, A. Laine, M. O'Keeffe and O. M. Yaghi, *Science*, 1999, **283**, 1145.

3 (*a*) E. Lee, J. Kim, J. Heo, D. Whang and K. Kim, *Angew. Chem., Int. Ed.*, 2001, **40**, 399; (*b*) J. J. Bodwin and V. L. Pecoraro, *Inorg. Chem.*, 2000, **39**, 3434; (*c*) V. L. Pecoraro, J. J. Bodwin and A. D. Cutland, *J. Solid State Chem.*, 2000, **152**, 68; (*d*) J. A. Brant, Y. Liu, D. F. Sava, D. Beauchamp and M. Eddaoudi, *J. Mol. Struct.*, 2006, **796**, 160; (*e*) Y. Zou, M. Park, S. Hong and M. S. Lah, *Chem. Commun.*, 2008, 2340; (*f*) J. J. Perry IV, V. C. Kravtsov, G. J. McManus and M. J. Zaworotko, *J. Am. Chem. Soc.*, 2007, **129**, 10076; (*g*) A. J. Cairns, J. A. Perman, L. Wojtas, V. C. Kravtsov, M. H. Alkordi, M. Eddaoudi and M. J. Zaworotko, *J. Am. Chem. Soc.*, 2008, **130**, 1560; (*h*)

P.-X. Yin, J. Zhang, J.-K. Cheng, Z.-J. Li and Y.-G. Yao, *Inorg. Chem. Commun.*, 2006, **9**, 541; (*i*) R. Wang, M. Hong, J. Luo, R. Cao and J. Weng, *Chem. Commun.*, 2003, 1018.

4 (*a*) J. Park, S. Hong, D. Moon, M. Park, K. Lee, S. Kang, Y. Zou, R. P. John, G. H. Kim and M. S. Lah, *Inorg. Chem.*, 2007, **46**, 10208; (*b*) F. Nouar, J. F. Eubank, T. Bousquet, L. Wojtas, M. J. Zaworotko and M. Eddaoudi, *J. Am. Chem. Soc.*, 2008, **130**, 1833.

5 D. Moon and M. S. Lah, *Inorg. Chem.*, 2005, **44**, 1934.

6 (*a*) M. Moon, I. Kim and M. S. Lah, *Inorg. Chem.*, 2000, **39**, 2710; (*b*) D. Moon, J. Song, B. J. Kim, B. J. Suh and M. S. Lah, *Inorg. Chem.*, 2004, **43**, 8230.

7 R. P. John, D. Moon and M. S. Lah, *Supramol. Chem.*, 2007, **19**, 295. The network, **1**, is a three-fold interpenetrating 3D net with 3-connected 4.8.16 topology.

8 (*a*) B. Kwak, H. Rhee and M. S. Lah, *Inorg. Chem.*, 1998, **37**, 3599; (*b*) B. Kwak, H. Rhee and M. S. Lah, *Polyhedron*, 2000, **19**, 1985; (*c*) R. P. John, K. Lee, B. J. Kim, B. J. Suh, H. Rhee and M. S. Lah, *Inorg. Chem.*, 2005, **44**, 7109; (*d*) R. P. John, J. Park, D. Moon, K. Lee and M. S. Lah, *Chem. Commun.*, 2006, 3699; (*e*) R. P. John, K. Lee and M. S. Lah, *Chem. Commun.*, 2004, 2660; (*f*) R. P. John, M. Park, D. Moon, K. Lee, S. Hong, Y. Zou, C. S. Hong and M. S. Lah, *J. Am. Chem. Soc.*, 2007, **129**, 14142; (*g*) K. Lee, R. P. John, M. Park, D. Moon, H.-C. Ri, G. H. Kim and M. S. Lah, *Dalton Trans.*, 2008, 131; (*h*) D. Moon, K. Lee, R. P. John, G. H. Kim, B. J. Suh and M. S. Lah, *Inorg. Chem.*, 2006, **45**, 7991; (*i*) S.-X. Liu, S. Lin, B.-Z. Lin, C.-C. Lin and J.-Q. Huang, *Angew. Chem.*, 2001, **113**, 1118; (*j*) S. Lin, S.-X. Liu, Z. Chen, B.-Z. Lin and S. Gao, *Inorg. Chem.*, 2004, **43**, 2222; (*k*) S. Lin, S.-X. Liu, J.-Q. Huang and C.-C. Lin, *J. Chem. Soc., Dalton Trans.*, 2002, 1595.

9 (*a*) M. O'Keeffe and S. T. Hyde, *Zeolites*, 1997, **19**, 370; (*b*) G. O. Brunner, *Zeolites*, 1993, **13**, 592; (*c*) R. J. Hill, D.-L. Long, N. R. Champness, P. Hubberstey and M. Schröder, *Acc. Chem. Res.*, 2005, **38**, 337.

10 Platon program (Ver 1.08): A. L. Spek, *Acta Crystallogr., Sect. A*, 1990, **46**, 194.

11 A. J. Arvai and C. Nielsen, *ADSC Quantum-210 ADX Program, Area Detector System Corporation*, Poway, CA, USA, 1983.

12 Z. Otwinowski and W. Minor, in *Methods in Enzymology*, ed. C. W. Carter, Jr. and R. M. Sweet, Academic Press, New York, 1997, vol. 276, (part A), pp. 307.

13 G. M. Sheldrick, *SHELXTL-PLUS, Crystal Structure Analysis Package*; Bruker Analytical X-Ray; Madison, WI, USA, 1997.

14 SMART and SAINT, *Area Detector Software Package and SAX Area detector Integration Program*, Bruker Analytical X-ray: Madison, WI, 1997.

15 SADABS, *Area Detector Absorption Correction Program*, Bruker Analytical X-ray: Madison, WI, 1997.